Mechanoresponsive resonance differences in double-network hydrogels towards multipartite dynamics

Ziyu Xing[1], Peizhao Li[1], Haibao Lu[1,3] and Yong Qing Fu[2,3]

[1]Science and Technology on Advanced Composites in Special Environments Laboratory, Harbin Institute of Technology, Harbin 150080, China

[2]Faculty of Engineering and Environment, Northumbria University, Newcastle upon Tyne, NE1 8ST, UK

[3]Corresponding author, E-mail: luhb@hit.edu.cn and richard.fu@northumbria.ac.uk

Abstract: Unlike single-network hydrogel whose thermodynamic equilibrium of all phases is governed by one single rule, double-network (DN) hydrogel is incorporated of two coexisting phases, which are separated from each other due to the differences in their mechanoresponsive responses. However, the resonance differences and multipartite dynamics of coexisting phases in these DN hydrogels have not been fully understood. This paper reports a new methodology to use a rheological model in combination of Arrhenius principle and Kirkwood approximation, to characterize the differences in mechanoresponsive resonances and viscoelastic behaviors of coexisting phases in the DN hydrogel. Their multipartite dynamics has been identified to originate from mechanical stretching, mechanochemical coupling and chemical kinetics of the ductile network, original brittle network and self-healed brittle network, respectively. Furthermore, molecular dynamics simulation and finite-element analysis have been conducted to verify the proposed model and explore the toughening mechanism, which is determined not only by the mechanochemical coupling, but also by the self-healing kinetics. Finally, effectiveness of proposed model has been well

verified using the experimental results of DN hydrogels reported in literature.

Keywords: double-network; hydrogel; coexisting phases; resonance difference

1. Introduction

Integration of active multi-networks with sacrificial bonds is one of the most popular approaches to enable the soft matter with both high mechanical strength and large deformation capability [1-7]. This approach makes a variety of materials such as polyelectrolyte [8], polyelectrolyte complex [9], polyion complexes [10] and double network (DN) hydrogels [11], with great potentials for artificial muscle, battery, soft robots, actuators, transducers and electronics [11-16]. Double-network (DN) hydrogels have recently attracted great attention due to their significantly improved mechanical properties in comparison with those of the conventional single-network (SN) hydrogels [17-22]. DN hydrogels are incorporated of two distinctive types of polymeric network components, e.g., the sacrificial one and ductile one, respectively [23,24]. The presence of sacrificial network resists the mechanical loading by means of bond broken [7-11]. Owing to their different viscoelastic responses of sacrificial and ductile networks, the DN hydrogels possess cooperative thermodynamics in response to an externally mechanical loading [25-27].

Previous studies have well characterized the mechanical behavior and toughening mechanism of DN hydrogels, and a series of phenomenological models have also been formulated to describe their mechanoresponsive behavior [28-32]. Furthermore, other types of DN hydrogels have been synthesized to improve the mechanical

performance using ionic bond, hydrogen bond, or monomer additive [7-11,33]. However, the working principle of resonance difference and multipartite dynamics of these complex coexisting phases in the DN hydrogels have yet been fully understood [34].

In this study, we propose an analytical model for the mechanoresponsive resonance differences in coexisting phases of DN hydrogel, which undergoes multipartite dynamics owing to the complex coexisting phases. A rheological model is firstly formulated for their differences of mechanoresponsive resonances and viscoelastic behaviors, in terms of the Arrhenius equation and Kirkwood approximation, to characterize the mechanochemical coupling and self-healing. Then, molecular dynamics (MD) simulation and finite-element analysis (FEA) have been conducted in order to explore the working principles of multipartite dynamics and toughening mechanisms in the DN hydrogels. Finally, the experimental data reported in literature have been employed to verify the effectiveness of the newly proposed model.

2. Theoretical framework

2.1 Extended rheological model

Hydrogels with a DN structure have been developed into many different material systems [7-11]. In the DN hydrogels, ductile network resists the externally mechanical loading depending on its stretchability, while the brittle one undergoes a mechanochemical transition and disperses the mechanical energy, as illustrated in Figure 1(a). These result in complex viscoelastic behaviors of DN hydrogels as shown

in Figure 1(b), where internal friction and friction viscosity are employed to characterize the mechanoresponsive differences between brittle and ductile networks.

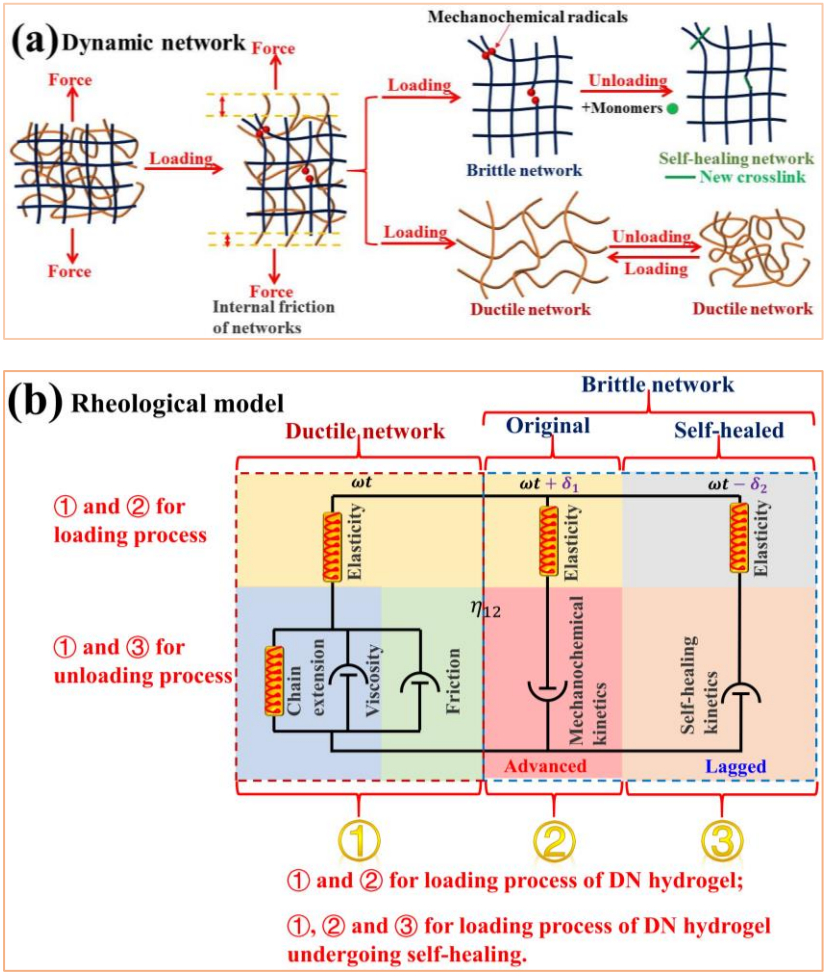

Figure 1. Schematic illustrations of mechanoresponsive behaviors and the viscoelastic rheological model of DN hydrogel. (a) Mechanoreponsive behaviors of dynamic networks. (b) Rheological model of dynamic networks.

According to the Maxwell principle [21,22], the constitutive stress-strain relationships for the ductile network, original brittle network and self-healed brittle network can be expressed as following, respectively,

$$\frac{d(\varepsilon-\varepsilon_v)}{dt}=\frac{1}{E_1}\frac{d\sigma_1}{dt} \tag{1a}$$

$$\sigma_1 = E_v\varepsilon_v + \eta_v\frac{d\varepsilon_v}{dt} + \eta_{12}\frac{d\varepsilon_v}{dt} \tag{1b}$$

$$\frac{d\varepsilon}{dt} = \frac{1}{E_2}\frac{d\sigma_2}{dt} - \frac{\sigma_2}{\eta_{12}} \tag{2}$$

$$\frac{d\varepsilon}{dt} = \frac{1}{E_3}\frac{d\sigma_3}{dt} + \frac{\sigma_3}{\eta_c} \tag{3}$$

where t is the time, σ and ε are the stress and strain of DN hydrogel. E_v, ε_v and η_v are the elastic modulus, strain and viscosity of the viscoelastic component in the ductile network, respectively. σ_1, σ_2 and σ_3 are the stresses of ductile, original brittle and self-healed brittle network, respectively. E_1, E_2 and E_3 are the moduli of ductile, original brittle and self-healed brittle networks, respectively. η_{12} is the viscosity of ductile and original brittle networks, and η_c is the viscosity of ductile and self-healed brittle networks. The equations (1), (2) and (3) can be rewritten as a function of strain or stretchable ratio ($\dot{\varepsilon}$, $\varepsilon = \dot{\varepsilon}t$),

$$\frac{\sigma_1}{\dot{\varepsilon}E_1\tau_1} = \frac{E_1}{E_1+E_v}[1-\exp(\frac{-\varepsilon}{\tau_1\dot{\varepsilon}})] + \frac{E_v}{E_1+E_v}\frac{\varepsilon}{\tau_1\dot{\varepsilon}} \tag{4}$$

$$\frac{\sigma_2}{\dot{\varepsilon}E_2\tau_2} = \exp(\frac{\varepsilon}{\tau_2\dot{\varepsilon}}) - 1 \tag{5}$$

$$\frac{\sigma_3}{\dot{\varepsilon}E_3\tau_3} = 1-\exp(\frac{-\varepsilon}{\tau_3\dot{\varepsilon}}) \tag{6}$$

where $\tau_1 = \frac{\eta_{12}+\eta_v}{E_1+E_v}$, $\tau_2 = \frac{\eta_{12}}{E_2}$ and $\tau_3 = \frac{\eta_c}{E_3}$ are relaxation times of ductile, original brittle and self-healed brittle networks, respectively. According to the chemical reaction kinetics [21,22], the broken (R_i) and termination (R_t) ratio of original brittle network can be obtained as,

$$R_i = 2f_ik_d\lceil I \rceil \tag{7}$$

$$R_t = 2k_t \lceil M\square \rceil^2 \tag{8}$$

where $\lceil I \rceil$ is the concentration of chains involved into the mechanochemical reaction, $\lceil M\square \rceil$ is the concentration of free radicals, f_i is the initiator concentration, k_d and k_i are the propagation rates of bond-broken and bond-polymerized, respectively. Therefore, the concentration of free radicals can be obtained as,

$$\lceil M\square \rceil = \sqrt{\frac{f_i k_d}{k_t} \lceil I \rceil} \tag{9}$$

where k_d is the chemical kinetics constant and ruled by the Arrhenius equation [21,22,35],

$$\begin{cases} k_d = A_d \exp(-\dfrac{E_d}{RT}) \\ k_t = A_t \exp(-\dfrac{E_t}{RT}) \end{cases} \tag{10}$$

where T is the temperature, R=8.314 J/K is the gas constant, E_d and E_t are the active energy values for bond breakage and polymerization, respectively. Both A_d and A_t are the constants. Substituting equation (10) into (9), the concentration of free radicals can be expressed as,

$$\lceil M\square \rceil = \sqrt{\frac{f_i A_d}{A_t} \lceil I \rceil} \exp(-\frac{\Delta E - k_\varepsilon \varepsilon}{2RT}) \tag{11}$$

where $\Delta E = E_d - E_t$. According to the rubber elastic theory [21,22], the modulus of original brittle network can be obtained as,

$$E_2 = \frac{n_{el} RT}{1 + \dfrac{\lceil M\square \rceil}{2\lceil I \rceil} \Delta V} = \frac{n_{el} RT}{1 + \dfrac{\Delta V}{2} \sqrt{\dfrac{f_i A_d}{A_t \lceil I \rceil}} \exp(-\dfrac{\Delta E - k_\varepsilon \varepsilon}{2RT})} \tag{12}$$

where n_{el} is the molar cross-linking density, ΔV is the volume change of original brittle network. Based on the Kirkwood approximation and Einstein model [36,37], the viscosity (η_c) of self-healing brittle network can be obtained as,

$$\frac{\eta_c-\eta_0}{\eta_0}\propto N_c^{\frac{4}{5}}=N_{c0}^{\frac{4}{5}}(1-\frac{\lceil M\rceil}{2\lceil I\rceil})^{\frac{4}{5}} \tag{13a}$$

$$\frac{\eta_c}{\eta_0}=k_\eta N_c^{\frac{4}{5}}+1=k_\eta N_{c0}^{\frac{4}{5}}[1-\frac{1}{2}\sqrt{\frac{f_iA_d}{A_t\lceil I\rceil}}\exp(-\frac{\Delta E-k_\varepsilon\varepsilon}{2RT})]^{\frac{4}{5}}+1 \tag{13b}$$

where η_0 is the initial viscosity, k_η is the scaling constant, N_{c0} and N_c are the initial and final chain numbers of self-healing brittle network, respectively.

In combination of equations (4), (5), (6), (11), (12) and (13), the constitutive stress-strain equation can be finally obtained,

$$\sigma=\sigma_1+\sigma_2+\sigma_3 \tag{14a}$$

$$\sigma_1=\frac{\dot\varepsilon E_1^2\tau_1}{E_1+E_v}[1-\exp(-\frac{\varepsilon}{\tau_1\dot\varepsilon})]+\frac{E_1E_v\varepsilon}{E_1+E_v} \tag{14b}$$

$$\frac{\sigma_2}{\dot\varepsilon\eta_{12}}=\exp(\frac{n_{el}RT\varepsilon/\dot\varepsilon\eta_{12}}{1+\frac{\Delta V}{2}\sqrt{\frac{f_iA_d}{A_t\lceil I\rceil}}\exp(-\frac{\Delta E-k_\varepsilon\varepsilon}{2RT})})-1 \tag{14c}$$

$$\frac{\sigma_3}{\dot\varepsilon\eta_c}=1-\exp(\frac{-E_3}{\eta_c}\frac{\varepsilon}{\dot\varepsilon}) \tag{14d}$$

$$\frac{\eta_c}{\eta_0}=k_\eta N_{c0}^{\frac{4}{5}}[1-\frac{1}{2}\sqrt{\frac{f_iA_d}{A_t\lceil I\rceil}}\exp(-\frac{\Delta E-k_\varepsilon\varepsilon}{2RT})]^{\frac{4}{5}}+1 \tag{14e}$$

In the rheological model, material parameters are determined based on the experimental measurement results in literature, i.e., R=8.314 J/K, k_B=1.38×10^{-23} J/K [21,22]; T=298.5 K [8,9,11]; $\dot\varepsilon$=0.0694 s^{-1} [8], 0.28 s^{-1} [9], 0.33 s^{-1} [11], respectively; the modulus is ranged from 0.01 MPa to 1 MPa [8,9,11]; ΔE=0.2RT J/mol and $\frac{f_iA_d}{A_t}$ is ranged from 1.0×10^{-4} to 1.0×10^4 [21,22].

2.2 MD simulation

A brittle network, which is incorporated from poly(2-acrylamido-2-methylpropane-sulfonic acid) (PAMPS) [11], is chosen to simulate the mechanochemical behavior using the MD simulation The chemical structures and atomistic representations of the PAMPS obtained from the MD simulation are presented in Figure 2(a). The PAMPS network consisting of 15 molecules with 420 atoms in total are generated by Amorphous Cell module implemented in Materials Studio, and the selected size is capable to reproduce the mechanical properties close to those of bulk cases. After the construction, the hydrogel system is equilibrated in canonical ensemble at a constant temperature of 298.5 K for 50 ps. While another equilibration process is carried out in the isoenergy ensemble with a room temperature of 298.5 K for 50 ps. The cell size of the model is 16.75×16.75×16.75 $Å^3$.

In the tensile tests, the simulation cell is deformed in a step-wise manner along z direction while the pressures along the other two directions are kept constants. The tensile deformation is performed in the isoenergy (NVE) ensemble at the end of the simulation with an applied pressure of 0.132 GPa and a total energy of 2091.787 kcal/mol. The applied stress is $\sigma=3k_BT\Delta h/h_0^2$ (k_B=1.38×10^{-23} J/K and h_0=1.675 nm) according to the rubber elasticity theory [21,22]. The theoretical results obtained using the equations (5) and (6) have also been presented in comparisons with those from the MD simulations, as shown in Figure 2(b). During the analysis, the following parameters are used in equations (5) and (6), e.g., $\dot{\varepsilon}E_2$=0.05707 pPa, $\dot{\varepsilon}E_3$=4.264 pPa,

τ_2=26.31 ps and τ_3=1.274 ps. After comparisons, it is revealed that the analytical results of our newly proposed model fit well with the MD simulation ones.

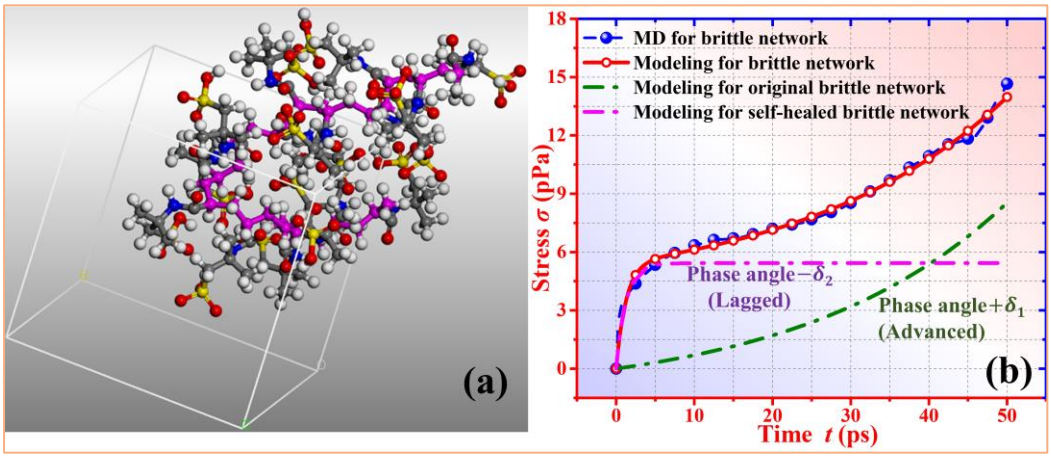

Figure 2. (a) Chemical and atomistic structures of PAMPS by MD simulation. (b) The change in stress as a function of time for PAMPS brittle network.

To verify the proposed model and identify the constitutive relationship of the applied force as a function of length, a group of experimental data of PNaAMPS/PAAm (PNaAMPS: poly(2-acrylamido-2-methylpropanesulfonic acid) sodium salt; PAAm: poly(acrylamide)) hydrogels reported in Ref. [11] have been employed to compare with the analytical results obtained using equation (14). The results are shown in Figure 3(a). The parameters used in the equation (14) are listed in Table 1, where T=298.5 K [11], R=8.314 J/K [22], $\eta_0 k_\eta N_{c0}^{\frac{4}{5}}$=0.31, E_3=0.0806 N, $\dot{\varepsilon}$ =0.33s^{-1} [11] and ΔE=0.2RT J/mol [21]. The analytical results fit well with the experimental data, and the proposed model can be used to characterize the mechanical behaviors of the PNaAMPS/PAAm DN hydrogel. With an increase in the mechanical cycle from 1st, 2nd, 3rd to 4th, the obtained forces are gradually increased from 1.42 N, 1.97 N, 2.99 N to 3.93 N at the same length of L=90 mm. Meanwhile, the divergences between analytical and experimental results of the PNaAMPS/PAAm DN

hydrogels are calculated using the correlation index (R^2), and the obtained results are R^2=98.88%, R^2=97.68%, R^2=98.10%, and R^2=98.49% for 1st, 2nd, 3rd and 4th mechanical loading, respectively, as shown in Figure 3(b).

Table 1. Values of parameters used in equation (14) for PNaAMPS/PAAm DN hydrogel.

	$\frac{E_1^2\tau_1}{E_1+E_v}(\mathrm{N\cdot s})$	$\frac{E_1E_v}{E_1+E_v}(\mathrm{N})$	$\tau_1(\mathrm{s})$	$\eta_{12}(\mathrm{N\cdot s})$	$\frac{\Delta V}{2}\sqrt{\frac{f_iA_d}{A_t\lceil I\rceil}}$	k_ε	$\frac{n_{el}RT}{\eta_{12}}(\mathrm{s^{-1}})$
1st	0.616	0.131	3.3	1.48	0.2	8200	0.508
2nd	0.551	0.209	12	2.64	0.2	6420	0.510
3rd	0.385	0.131	12	1.48	0.2	6200	0.567
4th	1.62	0.760	12	8.40	0.2	10400	0.568

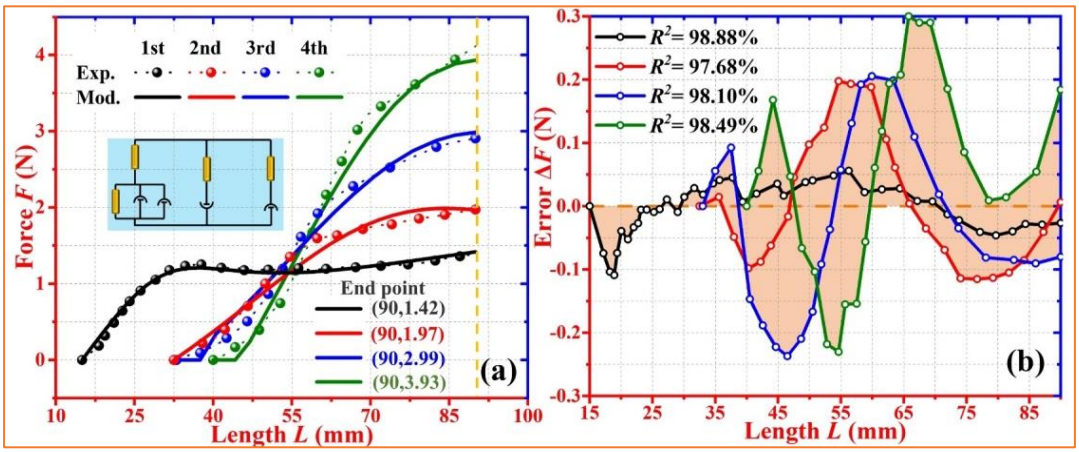

Figure 3. Comparisons of analytical and experimental results [11] for PNaAMPS/PAAm DN hydrogel undergoing self-healing in different mechanical cycles. (a) For the force-length curves. (b) Divergences of the analytical and experimental results.

3. Experimental verification

3.1 Multipartite dynamics in DN hydrogel

Experimental data [8] of PCDME/PAMPS (PCDME: poly-N-(carboxymethyl)-N, N-di-methyl-2-(methacryloyloxy) ethanaminium and PAMPS:

poly(2-acrylamido-2-methylpropane sulfonic acid)) DN hydrogel have been used to verify the analytical results generated from the proposed model. In the PCDME/PAMPS DN hydrogel, the PCDME acts as the ductile network, while the PAMPS works as the brittle one [8].

Figure 4(a) plots the constitutive stress-strain relationship of PCDME/PAMPS DN hydrogel with various PCDME/PAMPS molar ratios (R_m) of 10.5, 25.6 and 44.3. All the parameters used in the calculation using the equation (14) are listed in Table 2, at given constants of T=298.5 K [8], $\dot{\varepsilon}$=0.0694s^{-1} [8], R=8.314 J/K [22] and ΔE=0.2RT J/mol [21]. The experimental data [8] are employed to compare with the analytical results calculated using our model. With an increase in the PCDME/PAMPS molar ratio from 10.5, 25.6 to 44.3, the stress is gradually decreased from 1.07 MPa, 0.83 MPa to 0.66 MPa at the same strain of ε=1.5. With the increase of PCDME/PAMPS molar ratio, the stress decreases because of a lower molar ratio of PAMPS, which dissipates the mechanical energy. According to the experimental results [8], the PCDME works as the ductile network, while PAMPS acts as the brittle one and undergoes mechanochemical reaction. Experimental results reveal that the mechanical property of PCDME/PAMPS DN hydrogel is essentially determined by the PAMPS network, which undergoes mechanochemical reactions and thus dissipates the mechanical energy. Therefore, the stress is gradually decreased from 1.07 MPa, 0.83 MPa to 0.66 MPa at the same applied strain of ε=1.5, with an increase in the PCDME/PAMPS molar ratio from 10.5, 25.6 to 44.3. In Figure 4(b), the divergences between the analytical and experimental results are obtained by calculating the

correlation index (R^2), which are 92.28%, 99.79% and 99.37% at PCDME/PAMPS molar ratios (R_m) of 10.5, 25.6 and 44.3, respectively.

Table 2. Values of parameters used in equation (14) for PCDME/PAMPS DN hydrogel.

R_m	$\frac{E_1^2\tau_1}{E_1+E_v}$(MPa·s)	$\frac{E_1E_v}{E_1+E_v}$(MPa)	τ_1(s)	η_{12}(MPa·s)	$\frac{\Delta V}{2}\sqrt{\frac{f_iA_d}{A_t\lceil I\rceil}}$	k_ε	$\frac{n_{el}RT}{\eta_{12}}$(s^{-1})
10.5	0.001	0.532	901	3.72	0.171	1409	0.0478
25.6	1.65	0.199	20.1	6.57	24.03	4231	0.0862
44.3	0.001	0.211	0.357	1931	0.459	7580	0.000671

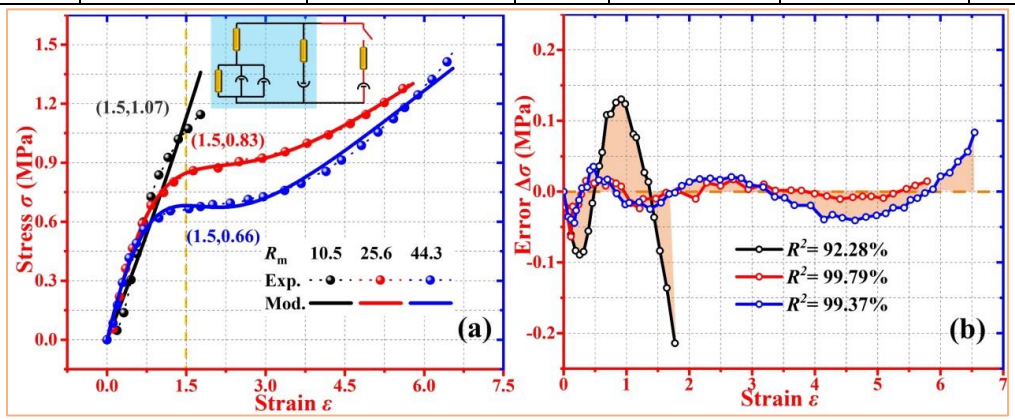

Figure 4. Analytical results and experimental data [8] of stress-strain curves of PCDME/PAMPS DN hydrogel, at the various PCDME/PAMPS molar ratio (R_m) of 10.5, 25.6 and 44.3. (a) The stress-strain curves. (b) Divergences of analytical and experimental results of stress.

Polyelectrolyte complex (PEC) DN hydrogel, which is incorporated from anionic poly(NaSS) (PNaSS) and cationic poly(diallyldimethyl-ammonium chloride) (PDADMAC) [9], has also been employed to verify the proposed model. In the PEC DN hydrogel, cationic PDADMAC acts as the ductile network, while the PNaSS acts as the brittle one [9]. Figure 5(a) plots the constitutive stress-strain relationship of the PEC DN hydrogels as a function of the molar fraction of anion (f). The parameters

used in the calculation using the equation (14) are listed in Table 3, at given constants of T=298.5 K [9], R=8.314 J/K [22], $\dot{\varepsilon}$=0.28s^{-1} [9] and ΔE=0.2RT J/mol [21]. The experimental data reported in Ref. [9] are employed to verify the analytical results obtained from our model.

Table 3. Values of parameters used in equation (14) for PEC DN hydrogel.

f	$\frac{E_1^2\tau_1}{E_1+E_v}$(MPa·s)	$\frac{E_1E_v}{E_1+E_v}$(MPa)	τ_1(s)	η_{12}(MPa·s)	$\frac{\Delta V}{2}\sqrt{\frac{f_iA_d}{A_t\lceil I\rceil}}$	k_ε	$\frac{n_{el}RT}{\eta_{12}}$(s^{-1})
0.45	5.625	0.516	0.256	0.357	371.1	3320	111.8
0.5	15.52	0.867	1.27×10^{-4}	0.357	3.928	43907	59.64
0.52	22.65	0.917	3.38×10^{-4}	0.357	102.4	36481	1101

Results show that the yielding stress is gradually increased from 1.38 MPa, 5.15 MPa to 7.03 MPa, with an increase in molar fraction of anion (f) from 0.45, 0.5 to 0.52, at the same strain of ε=0.1. Both the analytical and experimental results reveal that the mechanical yielding stress has been significantly enhanced with an increase in the molar fraction of anion (f), which is mainly due to the good mechanochemical properties of brittle network. With a higher molar fraction of anion (f), the brittle network, which is formed from the ionic bonds and undergoes the mechanochemical and self-healing transitions, is able to dissipate more mechanical energy into the chemical one. Therefore, the mechanical performance of the PEC DN hydrogel is improved with an increase in the molar fraction of anion (f). The divergences between the analytical and experimental results are calculated, and the obtained correlation index (R^2) are 99.98%, 99.93% and 99.96% for the PEC DN hydrogel with the molar fractions of anions of 0.45, 0.5 and 0.52, respectively, as shown in Figure 5(b). It can be clearly seen that the experimental data with various molar fractions of anions agree

well with the analytical results (|$\Delta\sigma$|<0.09 MPa).

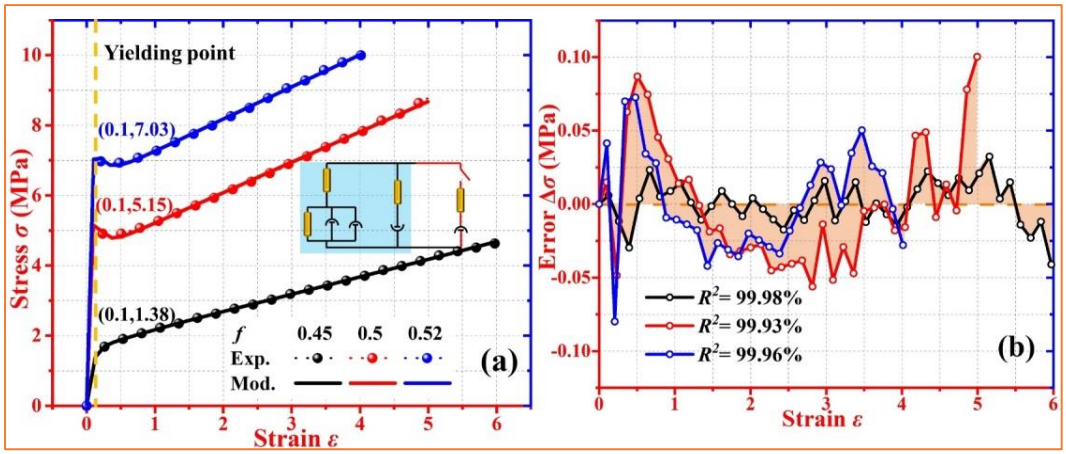

Figure 5. Analytical results and experimental data [9] of stress-strain curves of PEC DN hydrogel, at given molar fractions of anion of f=0.45, 0.5 and 0.52. (a) The stress-strain curves. (b) Divergences of analytical and experimental results of stress.

3.2 Mechanoresponsive resonance difference towards multipartite dynamics

The effect of resonance differences of coexisting phases on multipartite dynamics has been further investigated for the DN hydrogel. By introducing the parameter frequency response (ω) [21,22], the storage and loss moduli can be obtained as,

$$\begin{cases} E^{'} = E_1 \dfrac{\dfrac{E_v}{E_1+E_v}+\omega^2\tau_1^2}{1+\omega^2\tau_1^2} + E_2\dfrac{\omega^2\tau_2^2}{1+\omega^2\tau_2^2} + E_3\dfrac{\omega^2\tau_3^2}{1+\omega^2\tau_3^2} \\ E^{''} = E_1 \dfrac{\dfrac{E_1}{E_1+E_v}\omega\tau_1}{1+\omega^2\tau_1^2} - E_2\dfrac{\omega\tau_2}{1+\omega^2\tau_2^2} + E_3\dfrac{\omega\tau_3}{1+\omega^2\tau_3^2} \end{cases} \tag{15}$$

where $E^{'}$ and $E^{''}$ are the storage and loss moduli, respectively, and the phase angle (δ) is then obtained as $\delta = \arctan\dfrac{E^{''}}{E^{'}}$.

According to equation (15), the analytical results of storage and loss moduli of PEC DN hydrogel [9] have been obtained and are plotted as a function of frequency

response (ω) as shown in Figure 6. The parameters used in the equation (15) have been listed in Table 4. According to the time-temperature equivalence principle [21,22], the moduli as functions of relaxation time ($1/\omega$) and temperature (T) can be expressed as $E'(T, \omega)=E'(T_0, a_T\omega)$ and $E''(T, \omega)=E''(T_0, a_T\omega)$, respectively, where a_T is the shift factor. As shown in Figure 6(a), the analytical results obtained from our model fit well with the experimental data of the PEC DN hydrogel [9]. Meanwhile, Figure 6(b) shows the divergences between the analytical and experimental results calculated using the correlation index (R^2), which are 99.82% and 99.97% for storage and loss moduli, respectively.

Table 4. Values of parameters used in equation (16) for PEC DN hydrogel.

	E_1(MPa)	E_2(MPa)	E_3(MPa)	τ_1(s)	τ_2(s)	τ_3(s)	$E_v/(E_1+E_v)$	a_T
E'	0.03215	1.661	6.857	378.8	12.13	1.141	0.8693	0.434
E''	1.915	0.2708	2.468	0.1809	13.64	1.593	0.8693	0.302

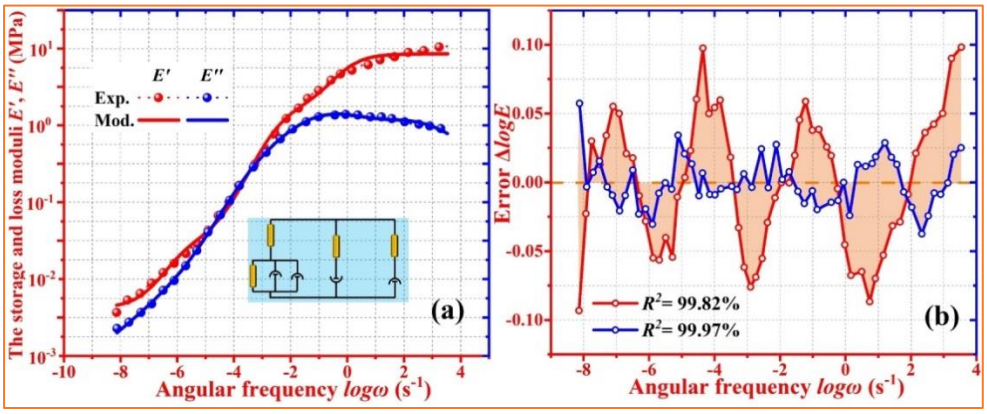

Figure 6. (a) Comparisons of analytical and experimental results [9] of storage and loss moduli of PEC DN hydrogel undergoing self-healing as a function of frequency response (ω). (b) Divergences of analytical and experimental results of storage and loss moduli.

In order to verify the validity of the model, the elastic theory of isotropic plate [38] is employed to characterize the mechanoresponsive resonance difference by deflection

($w = \pi \cdot \tan\delta = \pi \cdot \frac{E''}{E'}$), which can be obtained,

$$\omega_{ij} = \pi^2 \left(\frac{i^2}{a^2} + \frac{j^2}{b^2} \right) \sqrt{\frac{D}{\bar{m}}} \tag{16a}$$

$$w = \sum_{j=1}^{\infty} \sum_{i=1}^{\infty} \left(\frac{4w_0}{ab} \alpha_{ij} \cos\omega_{ij} t + \frac{4v_0}{ab} \frac{\alpha_{ij}}{\omega_{ij}} \sin\omega_{ij} t \right) \sin\frac{i\pi x}{a} \sin\frac{j\pi y}{b} \tag{16b}$$

where ω_{ij} is the frequency response, D is the bending stiffness, $\bar{m}$ is the mass per unit area, x and y are the position vectors ($x \in [0, a]$ and $y \in [0, b]$), $\alpha_{ij} = \int_0^a \int_0^b \sin\frac{i\pi x}{a} \sin\frac{j\pi y}{b} dxdy$, a and b are the length and width of the plates, w is the deflection, w_0 is the initial deflection, v_0 is the initial velocity, i and j are given integers where $i, j \in \{1, 2, \cdots\}$, respectively.

The model is used in simulations using ABAQUS. The same model is also used for both networks in the DN hydrogel, where the modulus of brittle network is 10 times than that of the flexible one according to experimental results [8,9,11]. In the case of free vibration, the Poisson's ratio and density are chosen as 0.45 and 0.8 g/cm^3, respectively, according to the rubber elastic theory [21,22]. A 20-node hexahedron element, C3D20R, was used to perform the calculation. About 2449 elements were used to model the unit and perform modal analysis.

FEA is firstly applied to analyze the mechanoresponsive resonance difference in the coexisting phases of DN hydrogel. As shown in Figure 7(a), there is a weak interaction between two networks, and the coexisting phases show a large resonance difference. On the other hand, the interaction between the two networks is strong, resulting in a small resonance difference of the coexisting phases, as shown in Figure

7(b). The FEA analysis results reveal that the mechanoresponsive resonance difference of coexisting phases enables a distinct deflection behavior of the networks, where a small resonance difference results into a slight deflection. Whereas a large resonance difference of coexisting phases results into a significant deflection of the networks. Therefore, the mechanoresponsive resonance difference and deflection of coexisting phases have been identified as the driving force to determine the mechanical behavior of DN hydrogel, and they are originated from the interaction between the two networks.

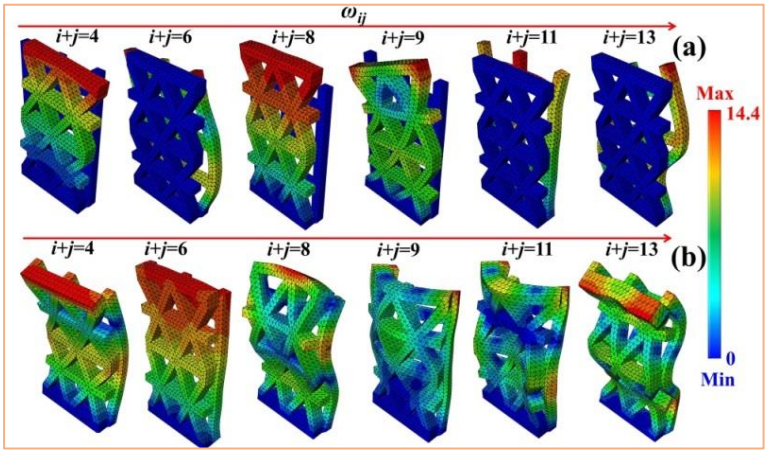

Figure 7. FEA of the mechanoresponsive resonance difference and deflection. (a) A large resonance difference in DN hydrogel undergoing an intense deflection. (b) A small resonance difference in DN hydrogel undergoing a slight deflection.

Furthermore, the effect of resonance difference on deflection has been investigated for the DN hydrogels. The following parameters $t=\frac{5}{24\pi}$, $\sqrt{D/\bar{m}}=1$, $a=b=1.0$ and $w_0=v_0=0.25$ are used in the calculation using the equation (16). The obtained 3D cloud chart, 2D cloud chart and deflection curves for the DN hydrogel are plotted in Figures 8(a), 8(b) and 8(c), respectively. When there is no interaction between coexisting

phases, an infinite resonance difference (ω_{ij} =∞) can be obtained. For comparisons, the 3D cloud chart, 2D cloud chart and deflection curves for the DN hydrogel have been plotted in Figures 8(d), 8(e) and 8(f), respectively. There is a weak interaction between coexisting phases, which results in an apparent resonance difference of $\omega_{ij} = \frac{2}{3}\pi^2$. Meanwhile, the 3D cloud chart, 2D cloud chart and deflection curves for the DN hydrogel have been plotted in Figures 8(g), 8(h) and 8(i), respectively, and there is a strong interaction between coexisting phases, which have resulted in a slight resonance difference of $\omega_{ij} = \frac{1}{3}\pi^2$.

These 2D cloud charts and deflection curves reveal that the mechanoresponsive deflection ($|w|$) has been significantly decreased from 0.11, 0.09 to 0.048 with a decrease in the resonance difference (ω_{ij}) from infinity, $\frac{2}{3}\pi^2$ to $\frac{1}{3}\pi^2$, due to the improved interaction between coexisting phases in the DN hydrogel. The mechanoresponsive deflection is significantly decreased due to the mechanochemical coupling and self-healing of the coexisting phases, which is due to the small resonance difference. Therefore, the toughening behavior is achieved in the DN hydrogel, whereas the working principle and toughening mechanism are originated from the mechanochemical coupling and self-healing of the brittle network.

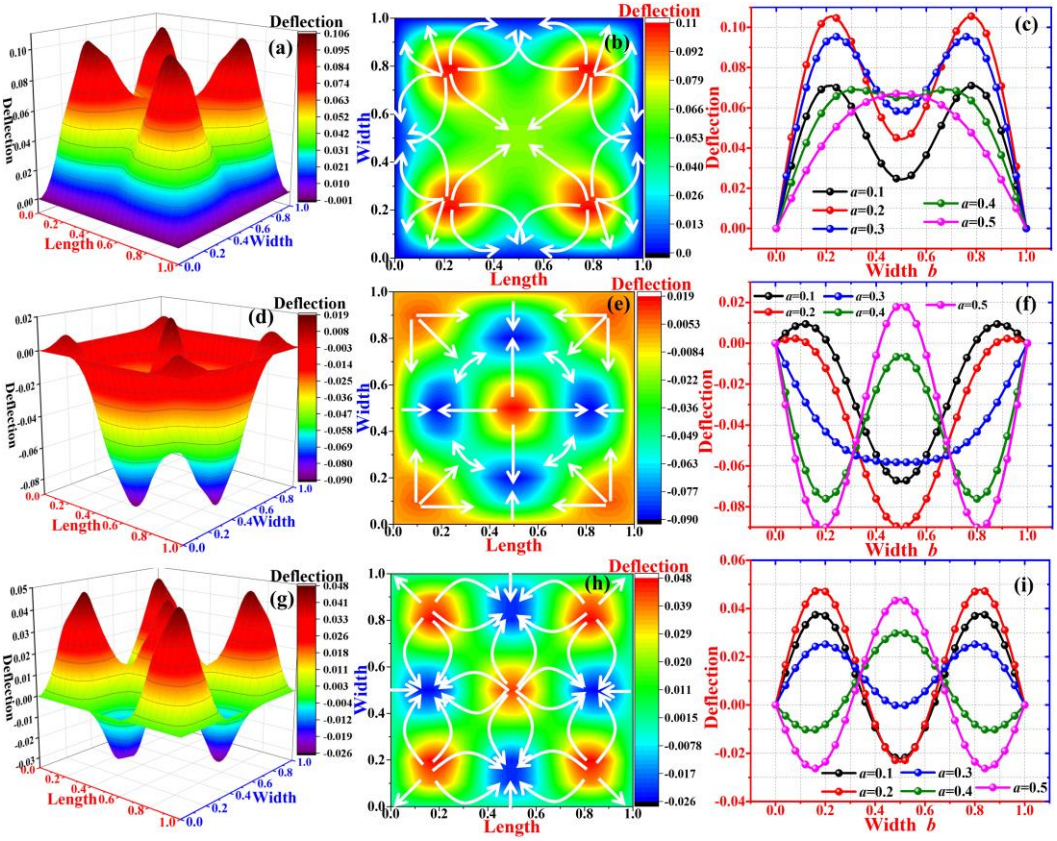

Figure 8. (a) 3D cloud chart, (b) 2D cloud chart and (c) deflection curves for the DN hydrogel, respectively, in which the coexisting phases undergo mechanical stretching at infinite resonance difference ($\omega_{ij}=\infty$). (d) 3D cloud chart, (e) 2D cloud chart and (f) deflection curves for the DN hydrogel, respectively, in which the coexisting phases undergo mechanical stretching and mechanochemical coupling at resonance difference of $\omega_{ij}=\frac{2}{3}\pi^2$. (g) 3D cloud chart, (h) 2D cloud chart and (i) deflection curves for the DN hydrogel, respectively, in which the coexisting phases undergo mechanical stretching, mechanochemical coupling and self-healing at resonance difference of $\omega_{ij}=\frac{1}{3}\pi^2$.

Furthermore, the effects of resonance difference (ω_{11}) and phase angle ($\delta=\omega_{11}t$) on deflection ($w=\pi\cdot\tan\delta=\pi\cdot\tan\omega_{11}t$) for the DN hydrogel have been further investigated,

and the obtained results are plotted in Figure 9, at the same relaxation time (t). During the analysis, the following parameters are used in equation (16), e.g., $\sqrt{D/\bar{m}}$=1, x=y=0.5, a=b=1 and w_0=v_0=0.25. It is revealed that the maximum deflection ($|w|$) of the DN hydrogel is gradually decreased from 0.69, 0.64 to 0.56, whereas the mechanochemical coupling and self-healing of the coexisting phases have been involved into the mechanoresponsive behavior. Furthermore, the mechanical energy has been slightly decreased, where the integral area is decreased from 0.4576, 0.4406 to 0.4321. These analytical results reveal that the DN hydrogel undergoes a small deflection while to dissipate the equally mechanical energy, due to the mechanochemical coupling and self-healing in combination of mechanical stretching of the coexisting phases.

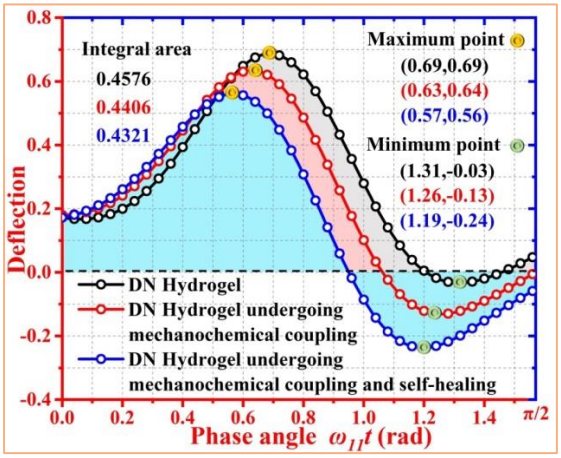

Figure 9. Analytical results of deflection as a function of phase angle for the DN hydrogel undergoing mechanochemical coupling and self-healing.

Moreover, these analytical results are also governed by the Maxwell principle [21,22]. The mechanochemical coupling and self-healing of the brittle network result in the viscoelastic behaviors to resist the mechanical force, which is in a parallel

connection with that of mechanical stretching of the ductile network. Therefore, the toughening of DN hydrogel is achieved by these viscoelastic branches.

4. Conclusions

In this study, we propose an extended rheological model for the mechanoresponsive resonance difference and viscoelastic behaviors of coexisting phases in the DN hydrogel, which undergoes multipartite dynamics of mechanical stretching, mechanochemical coupling and self-healing. The multipartite dynamics of coexisting phases has been identified as the driving force for the DN hydrogel due to their mechanoresponsive resonance differences. It is demonstrated that the proposed framework is able to well predict constitutive stress-strain relationship, creep test and thermodynamic behavior of DN hydrogels. Finally, FEA has been then carried out to explore the working principle of toughening mechanism, which has been significantly improved by the mechanochemical coupling and self-healing, resulting from the small resonance difference and slight deflection of coexisting phases. This study aims on understanding the multipartite dynamics and toughening mechanism of DN hydrogel, in terms of theoretical Maxwell principle, FEA analysis and experimental exemplification. It is expected that the formulated multi-field model of multipartite dynamics can be used to explore the working principle of mechanical behavior in DN hydrogels, undergoing complex chemical kinetics of mechanochemical coupling and self-healing.

Acknowledgements

This work was financially supported by the National Natural Science Foundation of China (NSFC) under Grant No. 11725208, and International Exchange Grant (IEC/NSFC/201078), through Royal Society and NFSC.

References

[1] Lin P, Ma S H, Wang X L and Zhou F 2015 Molecularly engineered dual-crosslinked hydrogel with ultrahigh mechanical strength, toughness and good self-recovery *Adv. Mater.* **27** 2054-9

[2] Fuchs S, Shariati K and Ma M 2020 Specialty tough hydrogels and their biomedical applications *Adv. Healthcare Mater.* **9** 1901396

[3] Sakai T, Matsunaga T, Yamamoto Y, Ito C, Yoshida R, Suzuki S, Sasaki N, Shibayama M and Chung U 2008 Design and fabrication of a high-strength hydrogel with ideally homogeneous network structure from tetrahedron-like macromonomers *Macromolecules* **41** 5379-84

[4] Gong J P, Katsuyama Y, Kurokawa T and Osada Y 2003 Double-network hydrogels with extremely high mechanical strength *Adv. Mater.* **15** 1155-8

[5] Haraguchi K and Takehisa T 2002 Nanocomposite hydrogels: a unique organic-inorganic network structure with extraordinary mechanical, optical, and swelling/de-Swelling properties *Adv. Mater.* **14** 1120-4

[6] Sun J Y, Zhao X, Illeperuma W R K, Chaudhuri O, Oh K H, Mooney D J, Vlassak J J and Suo Z 2012 Highly stretchable and tough hydrogels *Nature* **489** 133-6

[7] Zhang H J, Sun T L, Zhang A K, Ikura Y, Nakajima T, Nonoyama T, Kurokawa T, Ito O, Ishitobi H and Gong J P 2016 Tough physical double-network hydrogels based on amphiphilic triblock copolymers *Adv. Mater.* **28** 4884-90

[8] Yin H, King D R, Sun T L, Saruwatari Y, Nakajima T, Kurokawa T and Gong J P 2020 Polyzwitterions as a versatile building block of tough hydrogels: from polyelectrolyte complex gels to double-network gels *ACS Appl. Mater. Inter.* **12** 50068-76

[9] Murakawa K, King D R, Sun T L, Guo H, Kurokaw T and Gong J P 2019 Polyelectrolyte complexation via viscoelastic phase separation results in tough and self-recovering porous hydrogels *J. Mater. Chem. B.* **7** 5296-305

[10] Luo F, Sun T L, Nakajima T, Kurokawa T, Zhao Y, Sato K, Ihsan A B, Li X, Guo H and Gong J P 2015 Oppositely charged polyelectrolytes form tough, self-healing, and rebuildable hydrogels *Adv. Mater.* **27** 2722-7

[11] Matsuda T, Kawakami R, Namba R, Nakajima T and Gong J P 2019 Mechanoresponsive self-growing hydrogels inspired by muscle training *Science* **363** 504-8

[12] Huang Y, Li Z, Pei Z, Liu Z, Li H, Zhu M, Fan J, Dai Q, Zhang M, Dai L and Zhi C 2018 Solid-state rechargeable Zn//NiCo and Zn–Air batteries with ultralong lifetime and high capacity: the role of a sodium polyacrylate hydrogel electrolyte *Adv. Energy Mater.* **8** 1802288

[13] Zhang X, Yao D, Zhao W, Zhang R, Yu B, Ma G, Li Y, Hao D and Xu F J 2021 Engineering platelet-rich plasma based dual-network hydrogel as a bioactive wound dressing with potential clinical translational value *Adv. Funct. Mater.* **31** 2009258

[14] Yang C, Liu Z, Chen C, Shi K, Zhang L, Ju X J, Wang W, Xie R and Chu L Y 2017 Reduced graphene oxide-containing smart hydrogels with excellent

electro-response and mechanical properties for soft actuators *ACS Appl. Mater. Inter.* **9** 15758-67

[15] Fuhrer R, Athanassiou E K, Luechinger N A and Stark W J 2009 Crosslinking metal nanoparticles into the polymer backbone of hydrogels enables preparation of soft, magnetic field-driven actuators with muscle-like flexibility *Small* **5** 383-8

[16] Zheng W J, An N, Yang J H, Zhou J X and Chen Y M 2015 Tough Al-alginate/poly(N-isopropylacrylamide) hydrogel with tunable LCST for soft robotics *ACS Appl. Mater. Inter.* **7** 1758-64

[17] Sun T L, Luo F, Hong W, Cui K, Huang Y, Zhang H J, King D R, Kurokawa T, Nakajima T and Gong J P 2017 Bulk energy dissipation mechanism for the fracture of tough and self-healing hydrogels *Macromolecules* **50** 2923-31

[18] Cui K, Ye Y N, Sun T L, Liang C, Li X, Kurokawa T, Nakajima T, Nonoyama T and Gong J P 2019 Effect of structure heterogeneity on mechanical performance of physical polyampholytes hydrogels *Macromolecules* **52** 7369-78

[19] Chen Q, Chen H, Zhu L and Zheng J 2015 Fundamentals of double network hydrogels *J. Mater. Chem. B* **3** 3654-76

[20] Webber R E, Creton C, Brown H R and Gong J P 2007 Large strain hysteresis and Mullins effect of tough double-network hydrogels *Macromolecules* **40** 2919-27

[21] Fried J R 2014 *Polymer Science and Technology* (New Jersey: Prentice Hall)

[22] Flory P J 1953 *Principles of Polymer Chemistry* (New York: Cornell University Press)

[23] Yue Y F, Li X F, Kurokawa T and Gong J P 2016 Decoupling dual-stimuli responses in patterned lamellar hydrogels as photonic sensors *J. Mater. Chem. B.* **4** 4104-9

[24] Zheng S J, Li Z Q and Liu Z S 2019 The inhomogeneous diffusion of chemically crosslinked polyacrylamide hydrogel based on poroviscosity theory *Sci. China Technol. SC.* **62** 1375-84

[25] Tao L C, Sun L and Cui K P 2019 Facile synthesis of novel elastomers with tunable dynamics for toughness, self-healing and adhesion *J. Mater. Chem. A* **7** 17334-49

[26] Ahmed S, Nakajima T, Kurokawa K, Haque M A and Gong J P 2014 Brittleeductile transition of double network hydrogels: mechanical balance of two networks as the key factor *Polymer* **55** 914-23

[27] Ilyas M, Haque M A and Yue Y F 2017 Water-triggered ductile-brittle transition of anisotropic lamellar hydrogels and effect of confinement on polymer dynamics *Macromolecules* **50** 8169-77

[28] Nakajima T, Chida T, Mito K, Kurokawa T and Gong J P 2020 Double-network gels as polyelectrolyte gels with salt-insensitive swelling properties *Soft Matter* **16** 5487-96

[29] Nakajima T, Kurokawa T, Furukawa H and Gong J P 2020 Effect of the constituent networks of double-network gels on their mechanical properties and energy dissipation process *Soft Matter* **16** 8618-27

[30] Zhong D, Xiang Y, Liu J, Chen Z, Zhou H, Yu H, Qu S and Yang W 2020 A constitutive model for multi network elastomers pre-stretched by swelling *Extreme Mech. Lett.* **40** 100926

[31] Xing Z Y, Lu H B, Hossain M, Fu Y Q, Leng J S and Du S Y 2020 Cooperative dynamics of heuristic swelling and inhibitive micellization in double-network hydrogels by ionic dissociation of polyelectrolyte *Polymer* **186** 122039

[32] Lu H B, Xing Z Y, Hossain M and Fu Y Q 2019 Modeling strategy for dynamic-modal mechanophore in double-network hydrogel composites with self-growing and tailorable mechanical strength *Compos. Part B-Eng.* **179** 107528

[33] Gao H, Wang N, Hu X, Nan W, Han Y and Liu W 2012 Double hydrogen-bonding pH-sensitive hydrogels retaining high-strengths over a wide pH range *Macromol. Rapid Commun.* **34** 63-8

[34] Mao Y, Lin S, Zhao X and Anand L 2017 A large deformation viscoelastic model for double-network hydrogels *J. Mech. Phys. Solids* **100** 103-30

[35] Beyer M K and Clausen-Schaumann H 2005 Mechanochemistry: the mechanical activation of covalent bonds *Chem. Rev.* **105** 2921-48

[36] Landau S L and Lifshitz I 1959 *Fluid Mechanics* (London: Pergamon Press)

[37] Gennes P G 1979 *Scaling Concepts in Polymer Physics* (Ithaca and London: Cornell University Press)

[38] Reddy J N 2009 *Theory and Analysis of Elastic Plates and Shells* (Boca Raton: CRC Press)